Tissue-specific disruption of *Kbtbd2* uncovers adipocyte-intrinsic and -extrinsic features of the *teeny* lipodystrophy syndrome

Zhao Zhang[a,1], Thomas Gallagher[a], Philipp E. Scherer[b], and Bruce Beutler[a,1]

[a]Center for the Genetics of Host Defense, University of Texas Southwestern Medical Center, Dallas, TX 75390; and [b]Touchstone Diabetes Center, Department of Internal Medicine, University of Texas Southwestern Medical Center, Dallas, TX 75390

Contributed by Bruce Beutler, February 17, 2020 (sent for review January 6, 2020; reviewed by Silvia Corvera and Stephen O'Rahilly)

Loss of KBTBD2 in all tissues causes the *teeny* phenotype, characterized by insulin resistance with late failure of insulin production, severe hyperglycemia/diabetes, lipodystrophy, hepatosteatosis, and growth retardation. KBTBD2 maintains insulin sensitivity in adipocytes by restricting the abundance of p85α. However, the possible physiological contribution or contributions of KBTBD2 have not yet been examined in other tissues. Here we show that mice with an adipocyte-specific knockout of *Kbtbd2* accumulate p85α in white and brown adipose tissues, causing insulin resistance, moderate rather than severe hyperglycemia, sustained hyperinsulinemia without late failure of insulin production, and lipodystrophy leading to ectopic lipid accumulation in the liver. Adipocyte-extrinsic insulin resistance was observed in liver and muscle. None of these abnormalities were observed in liver- or muscle-specific *Kbtbd2* knockout mice. Mice with *Kbtbd2* knockout in adipocytes, liver, and muscle all showed normal growth, suggesting that KBTBD2 may be necessary to ensure IGF1 signaling in other tissues, notably bone. While much of the *teeny* phenotype results from loss of KBTBD2 in adipocytes, some features are adipocyte-extrinsic.

KBTBD2 | p85a | adipocytes | diabetes | insulin resistance

Insulin signaling is essential for the development and function of adipose tissue (1). Insulin drives the differentiation of preadipocytes to adipocytes by allowing glucose uptake and de novo triglyceride synthesis. Defects in differentiation of adipocytes or triglyceride synthesis cause a near-complete absence of adipose tissue, termed lipodystrophy. The binding of insulin to the insulin receptor (IR) activates the IR β subunit, which phosphorylates IR substrates IRS1 and IRS2, causing the activation of the phosphatidylinositol 3-kinase (PI3K) and the downstream AKT pathway (2), which, among other things, permits the up-regulation of glucose transporters on the surface of insulin-sensitive cells. Somewhat paradoxically, lipodystrophy can also be caused by tissue-specific insulin resistance, which can itself cause generalized insulin resistance and diabetes.

Recently we detected a phenotype termed *teeny* among third-generation C57BL/6J mice homozygous for *N*-ethyl-*N*-nitrosourea-induced mutations (3). The *teeny* phenotype is characterized by growth retardation, lipodystrophy, extreme insulin resistance, severe diabetes (with a fasting glucose level as high as 600 to 700 mg/dL), and hepatosteatosis. The causative mutation created a premature stop codon within *Kbtbd2*, which encodes a Kelch repeat and BTB (POZ)-domain containing protein. KBTBD2 functions together with CULLIN3 (CUL3) as an E3 ubiquitin ligase complex targeting p85α, the regulatory subunit of PI3K (3). Loss of KBTBD2 leads to a 30-fold accumulation of p85α in adipocytes (3). The excess monomeric p85α inhibits the insulin signaling pathway through competition with p85α-p110 for binding to IRS1 (3) and formation of a sequestration complex between p85α and IRS1 (4). Loss of KBTBD2 causes lipodystrophy, suggesting the importance of KBTBD2 in adipose tissue development. However, although transplantation studies suggested that some aspects of the *teeny* phenotype were adipocyte-intrinsic (3), expression of *Kbtbd2* mRNA is observed in other insulin-responsive tissues (e.g., muscle and liver) that are less readily evaluated through transplantation. Loss of KBTBD2 from these tissues might contribute to the *teeny* phenotype as well.

To determine the essential functions of KBTBD2 in specific tissues, we generated conditional knockout alleles activated by *cre* recombinase in three major insulin responsive tissues: adipose tissue, muscle, and liver. We find that loss of KBTBD2 in adipocytes is sufficient to cause lipodystrophy, hepatosteatosis, insulin resistance, and hyperglycemia. However, hyperglycemia was less severe than that observed in the *teeny* homozygotes, and late failure of insulin production was not observed, as it was in *teeny* homozygotes. Isolated conditional knockouts of *Kbtbd2* in adipose, muscle, or liver tissues was not sufficient to cause growth retardation, which remains unexplained.

Results

Generation of *Kbtbd2* Conditional Knockout Mice. To study the role of KBTBD2 in different tissues, we used CRISPR/Cas9-mediated gene editing to create a conditional knockout allele of *Kbtbd2* with exon 3 (Ex3) flanked by *LoxP* sites (*Kbtbd2-floxed*) (Fig. 1*A*). Ex3 of *Kbtbd2* contains a 166-bp sequence encoding amino acids 57 to 112 of the 623-amino acid KBTBD2 protein. The removal of Ex3 caused a deletion and frameshift, resulting in a null allele (Fig. 1*A*). Two different CRISPR sgRNAs (#1, #2) that targeted the left and right flanking introns of Ex3 were coinjected with two 200-bp oligo DNA templates into C57BL/6J

Significance

To examine the function of KBTBD2 in different cell types, we knocked the gene out in adipocytes, liver, and muscle cells. None of these conditional knockouts could reproduce the growth retardation observed in mice with a global knockout. An adipose tissue-specific knockout was similar to a global knockout in most respects; however, hyperglycemia was less severe and hyperinsulinemia was more sustained. An adipose tissue-specific knockout caused insulin resistance in other tissues, demonstrating an adipose-extrinsic effect of the mutation.

Author contributions: Z.Z. and B.B. designed research; Z.Z. performed research; Z.Z., P.E.S., and B.B. contributed new reagents/analytic tools; Z.Z. and B.B. analyzed data; and Z.Z., T.G., P.E.S., and B.B. wrote the paper.

Reviewers: S.C., University of Massachusetts Medical School; and S.O., University of Cambridge.

The authors declare no competing interest.

[1]To whom correspondence may be addressed. Email: Zhao.Zhang@UTSouthwestern.edu or Bruce.Beutler@UTSouthwestern.edu.

This article contains supporting information online at https://www.pnas.org/lookup/suppl/doi:10.1073/pnas.2000118117/-/DCSupplemental.

First published May 7, 2020.

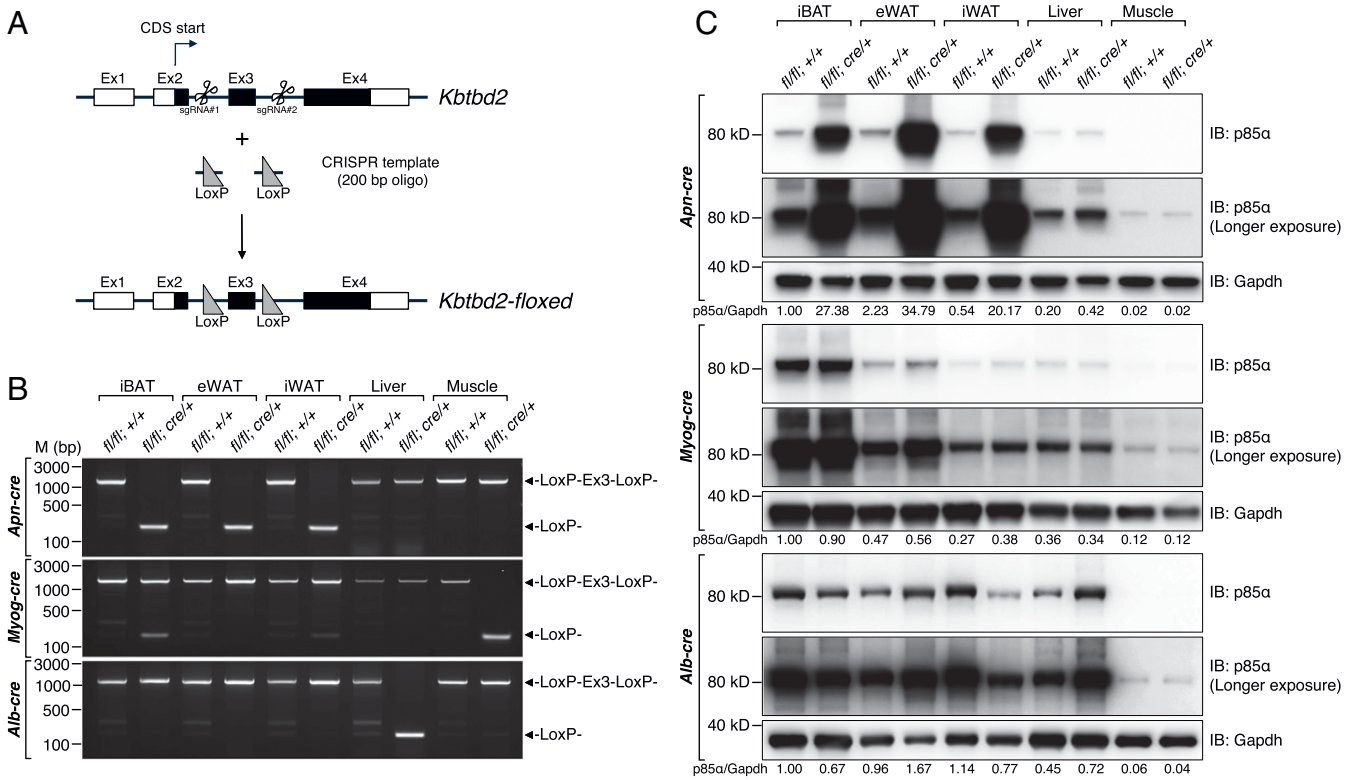

Fig. 1. Design and verification of tissue-specific *Kbtbd2* knockout mice. (*A*) Generation of *Kbtbd2-floxed* mice by CRISPR/Cas9-mediated gene replacement. (*B*) DNA agarose gels of genomic DNA PCR results showing the deletion of Ex3 in various tissues of $Kbtbd2^{flox/flox}$;*cre* mice compared with the intact Ex3 in $Kbtbd2^{flox/flox}$ littermates. (*C*) Immunoblots of different tissue lysates of $Kbtbd2^{flox/flox}$;*cre* mice and $Kbtbd2^{flox/flox}$ littermates. Quantification of bands are shown as the relative ratio of Integrated Density (IntDen) of p85α to Gapdh and the ratio for iBAT *fl/fl*;+/+ was set to 1.00 to allow for relative comparisons. IntDen was calculated with Image J 1.52q. Data are representative of two independent experiments.

zygotes (Fig. 1*A*). The *Kbtbd2-floxed* mice were crossed to different promoter-driven *cre*-recombinase transgenic mice to disrupt *Kbtbd2* in specific tissues. *Adiponectin* promoter-driven *cre*-recombinase (*Apn-cre*) (5) caused a specific deletion of Ex3 in interscapular brown adipose tissue (iBAT), epididymal white adipose tissue (eWAT), and inguinal white adipose tissue (iWAT; Fig. 1*B*). *Myogenin* promoter-driven *cre*-recombinase (*Myog-cre*) (6) caused a specific deletion of Ex3 in skeletal muscle (Fig. 1*B*). *Albumin* promoter-driven *cre*-recombinase (*Alb-cre*) (7) caused a specific deletion of Ex3 in liver (Fig. 1*B*). After successful generation of these tissue-specific *Kbtbd2* knockout models, we examined the accumulation of p85α, which is the direct target of KBTBD2 E3 ubiquitin ligase (3), in each of the three tissues. Loss of KBTBD2 in adipocytes caused a dramatic accumulation of p85α in all three adipose tissues tested (iBAT, eWAT, and iWAT), with no obvious change of p85α levels in liver and muscle (Fig. 1*C*). We separated adipose tissue into floating adipocytes and the stromal vascular fraction (SVF) (*SI Appendix*, Fig. S1*A*) and observed a specific accumulation of p85α in adipocytes, but not in the SVF (*SI Appendix*, Fig. S1*B*). Loss of KBTBD2 in skeletal muscle did not change the level of p85α in muscle, adipose tissues, or liver (Fig. 1*C*). In liver-specific *Kbtbd2* knockout mice, there was a slight increase in liver p85α, but not in adipose or muscle tissues (Fig. 1*C*). These data suggest cell-intrinsic degradation of p85α by KBTBD2 in adipocytes, and to a much lesser extent, hepatocytes.

Loss of KBTBD2 in Adipocytes Causes Lipodystrophy, but Not Growth Retardation. Growth retardation was observed in *teeny* and $Kbtbd2^{-/-}$ mice within the first few days and throughout postnatal life (3). We first examined whether any of the tissue-specific *Kbtbd2* knockouts contribute to the growth defect. In contrast to 8-wk-old $Kbtbd2^{-/-}$ mice, loss of *Kbtbd2* in adipose tissue, muscle, or liver did not affect the body weight (Fig. 2*A*) or body length (Fig. 2*B*), suggesting that KBTBD2 may affect growth through its function in other tissue or tissues.

A congenital systemic *Kbtbd2* knockout causes severe lipodystrophy (3), but it is not known whether the lipodystrophy is caused by the function of KBTBD2 in adipose tissue, muscle, liver, or a combination of these tissues. At 8 wk of age, MRI showed that only adipocyte-specific *Kbtbd2* knockout mice were as lean as $Kbtbd2^{-/-}$ mice (Fig. 2 *C* and *D* and *SI Appendix*, Fig. S2). No changes in fat weight or lean weight were observed in muscle-specific *Kbtbd2* knockout mice. Although the fat weight of liver-specific *Kbtbd2* knockout mice was slightly increased, this difference did not reach statistical significance (Fig. 2*C* and *SI Appendix*, Fig. S2*A*). Consistent with the body composition result, adipocyte-specific *Kbtbd2* knockout mice had reduced leptin and adiponectin in the serum, presumably as a consequence of fat loss (Fig. 2 *E* and *F*). No changes in leptin and adiponectin were observed in muscle-specific *Kbtbd2* knockout mice (Fig. 2 *E* and *F*). We also observed slightly increased leptin and adiponectin levels in liver-specific *Kbtbd2* knockout mice (Fig. 2 *E* and *F*), although similar to the change in fat mass measured by MRI, these changes were not statistically significant.

Necropsy revealed that both eWAT and iWAT of 16-wk-old adipocyte-specific *Kbtbd2* knockout mice were reduced in size compared with $Kbtbd2^{flox/flox}$ littermates (Fig. 2 *H* and *I*), with only a slight reduction in iBAT (Fig. 2*G*). Hematoxylin and eosin (H&E) staining revealed slightly irregular adipocytes in iBAT of

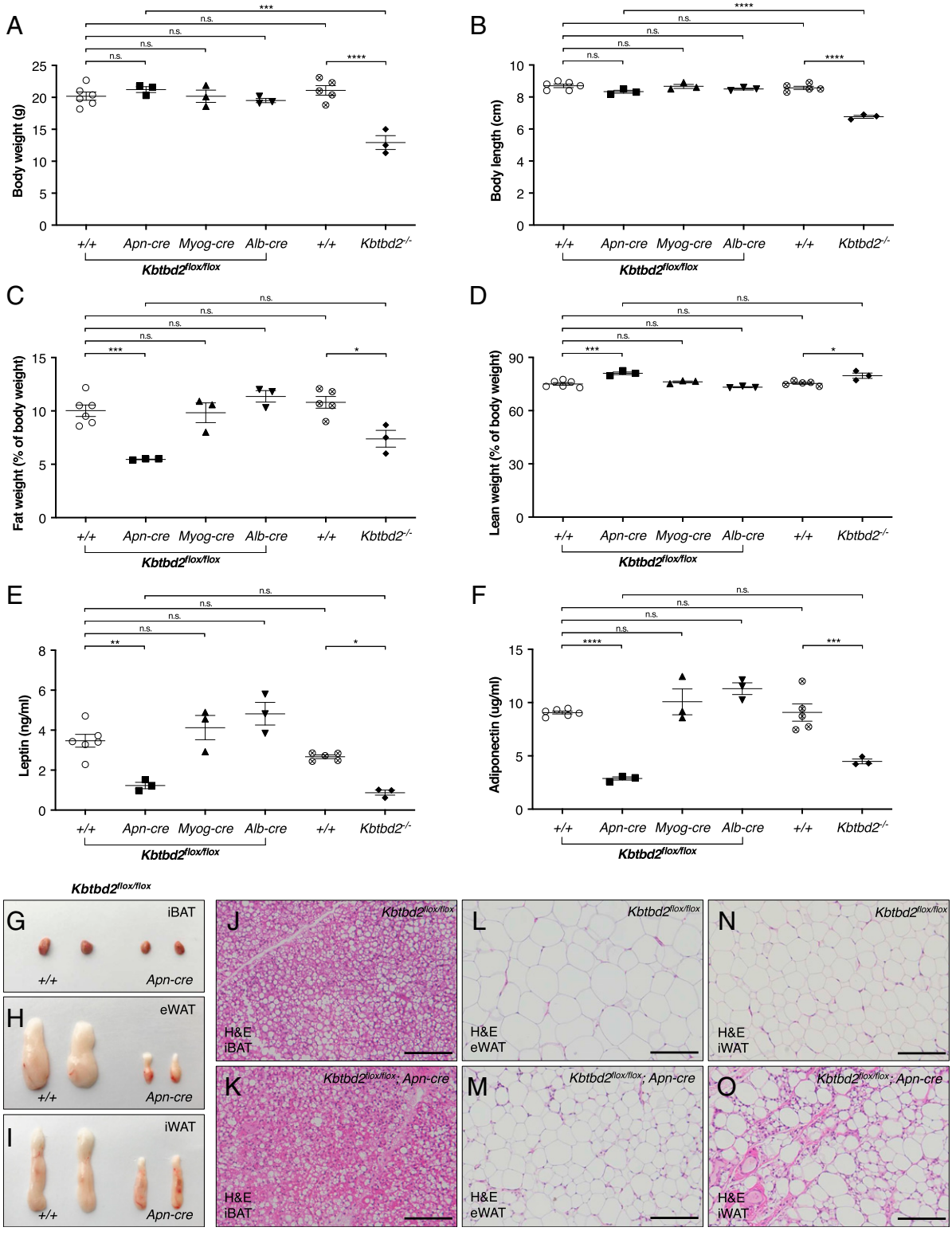

Fig. 2. Adipocyte-specific *Kbtbd2* knockout mice develop lipodystrophy despite having a normal growth rate. (*A*–*D*) Body weight (*A*), body length (*B*), fat weight (*C*), and lean weight (*D*) of 8-wk-old male mice. (*E*–*F*) Serum leptin (*E*) and adiponectin (*F*) of 8-wk-old male mice after a 6-h fast. (*G*–*I*) Representative photographs of iBAT (*G*), eWAT (*H*), and iWAT (*I*) from 16-wk-old male mice. (*J*–*O*) H&E staining of sections from different adipose tissues of 16-wk-old male mice. (Scale bar: 100 μm.) Data are representative of two independent experiments (*A*–*I*) or one experiment (*J*–*O*). Data points represent individual mice (*A*–*F*). Data are presented as means ± SEM (*A*–*F*). *P* values were determined by one-way ANOVA with Tukey's multiple comparison test. $*P \leq 0.05$; $**P \leq 0.01$; $***P \leq 0.001$; $****P \leq 0.0001$; ns, not significant with $P > 0.05$.

16-wk-old adipocyte-specific *Kbtbd2* knockout mice (Fig. 2 *J* and *K*). The eWAT and iWAT of these mice had irregular adipocytes with infiltration of nonfat cells (Fig. 2 *L*–*O*). We also noticed a larger variation in the size of adipocytes in both eWAT and iWAT of adipocyte-specific *Kbtbd2* knockout mice, suggesting the heterogeneity of adipocytes within adipose tissues. These data demonstrate that KBTBD2 functions directly in adipocytes either to maintain the mass of adipose tissues or is developmentally important for the generation of adipose tissue.

Loss of KBTBD2 in Adipocytes Causes Hepatosteatosis. Hepatosteatosis is another phenotype observed in *Kbtbd2* knockout mice (3). We utilized different *Kbtbd2* tissue-specific knockout mice to explore the exact role of KBTBD2 deficiency in the development of hepatosteatosis. Despite the high expression of *Kbtbd2* mRNA and protein in liver (3), knockout of *Kbtbd2* in adipocytes caused large and pallid fatty livers in 16-wk-old mice, but knockout in the liver or muscle did not (Fig. 3 *A*–*D*). Similarly, knockout of *Kbtbd2* only in adipocytes increased levels in serum alanine aminotransferase (ALT), which is an indication of liver damage (Fig. 3*E*). Histological analysis of the livers by H&E and Oil Red O staining likewise showed that only knockout of *Kbtbd2* in adipocytes caused increased lipid accumulation in the tissue (Fig. 3 *F*–*M*). Taken together, these findings clearly indicate that the hepatosteatosis in *Kbtbd2* knockout mice is a consequence of the loss of KBTBD2 in adipocytes. This is consistent with the frequently observed hepatic steatosis characteristic of most partial lipodystrophies. Notably, hepatosteatosis was not observed in mice with conditional knockouts of *Kbtbd2* in liver or muscle.

The Role of KBTBD2 in Glucose Metabolism and Insulin Sensitivity. Adipose tissue, liver, and muscle are insulin-responsive tissues. We used *Kbtbd2* tissue-specific knockout mice to directly determine whether systemic insulin sensitivity was dependent on KBTBD2 in adipose, muscle, or liver tissue, and whether the dependence was cell-intrinsic in each case. Only adipocyte-specific *Kbtbd2* knockout mice had elevated fasting glucose and insulin levels (Fig. 4 *A* and *B*). In contrast to *Kbtbd2*$^{-/-}$ mice, which have a persistent high fasting glucose level around 600 to 700 mg/dL (Fig. 4*A*, *SI Appendix*, Fig. S3*A*, and ref. 3), adipocyte-specific *Kbtbd2* knockout mice had a significantly smaller increase in fasting glucose, which reached around 300 to 400 mg/dL (Fig. 4*A* and *SI Appendix*, Fig. S3*A*). The increased fasting insulin level was similar to that observed in *Kbtbd2*$^{-/-}$ mice at 8 wk of age (Fig. 4*B*). However, we did not observe a decline in insulin levels in adipocyte-specific *Kbtbd2* knockout mice at 16 wk of age, as we previously observed in *Kbtbd2*$^{-/-}$ mice (*SI Appendix*, Fig. S3*A* and ref. 3). Insulin tolerance tests showed dramatic whole-body insulin resistance in adipocyte-specific *Kbtbd2* knockout mice, but not in muscle- or liver-specific *Kbtbd2* knockout mice (Fig. 4 *C*–*E*). We also tested the insulin sensitivity of eWAT, muscle, and liver by examining insulin-stimulated AKT phosphorylation at Ser-473 (p-AKT^{S473}). Adipocyte-specific *Kbtbd2* knockout mice had impaired insulin-stimulated p-AKT^{S473} in eWAT, as well as in muscle and liver (Fig. 4*F*). We did not observe a change in insulin-stimulated p-AKT^{S473} in muscle- and liver-specific *Kbtbd2* knockout mice (Fig. 4 *G* and *H*). These data suggest that KBTBD2 in adipocytes is critical for maintaining glucose metabolism and insulin sensitivity, and that loss of KBTBD2 in adipocytes also causes insulin resistance in liver and muscle.

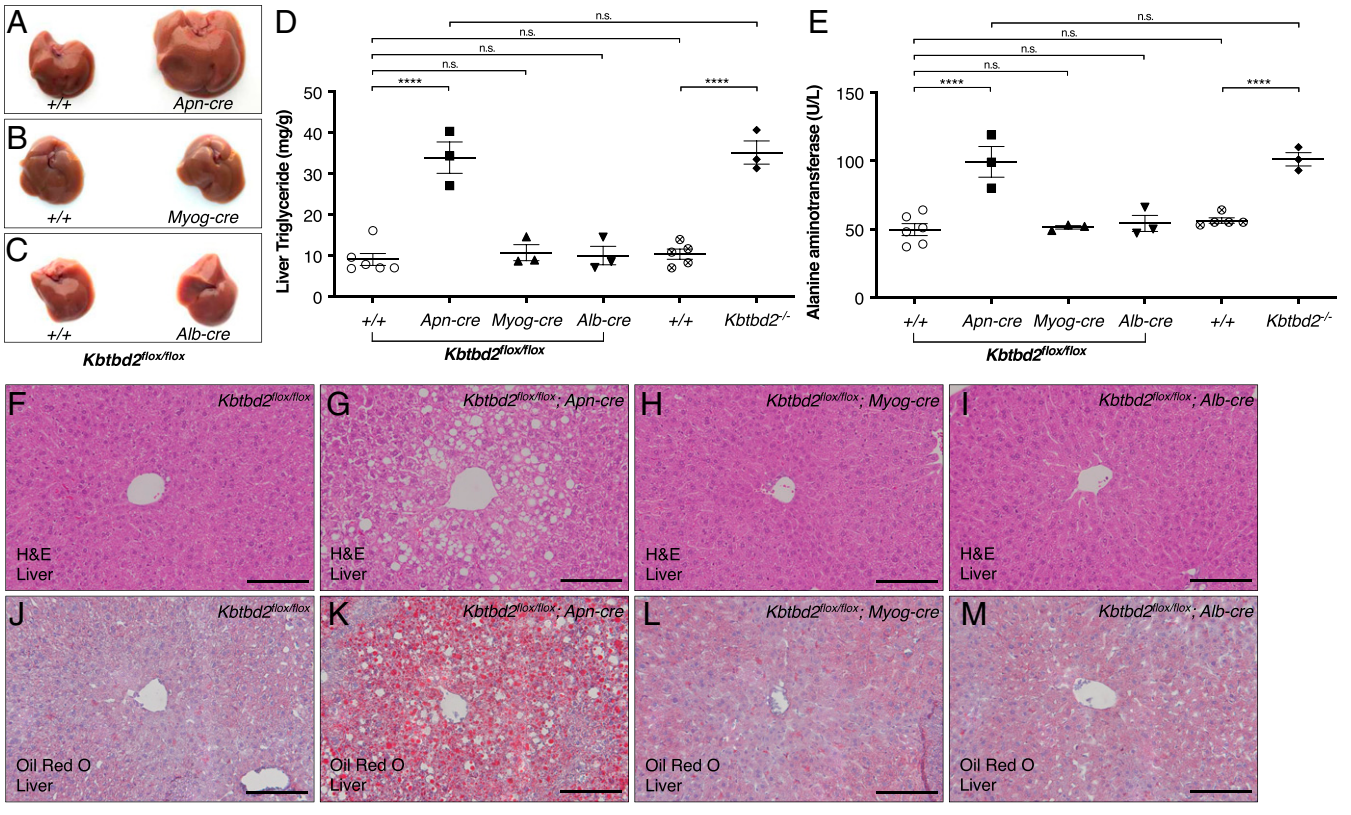

Fig. 3. Loss of *Kbtbd2* in adipocytes causes liver triglyceride accumulation and damage. (*A*–*C*) Representative photographs of liver from 16-wk-old male mice. (*D*–*E*) Liver triglyceride (*D*) and serum ALT (*E*) in 16-wk-old male mice. (*F*–*M*) Liver sections of 16-wk-old male mice stained with H&E (*F*–*I*) and Oil Red O (*J*–*M*). (Scale bar: 100 μm.) Data are representative of two independent experiments (*A*–*E*) or one experiment (*F*–*M*). Data points represent individual mice (*D*–*E*). Data are presented as means ± SEM (*D*–*E*). *P* values were determined by one-way ANOVA with Tukey's multiple comparison test. **P* ≤ 0.05; ***P* ≤ 0.01; ****P* ≤ 0.001; *****P* ≤ 0.0001; ns, not significant with *P* > 0.05.

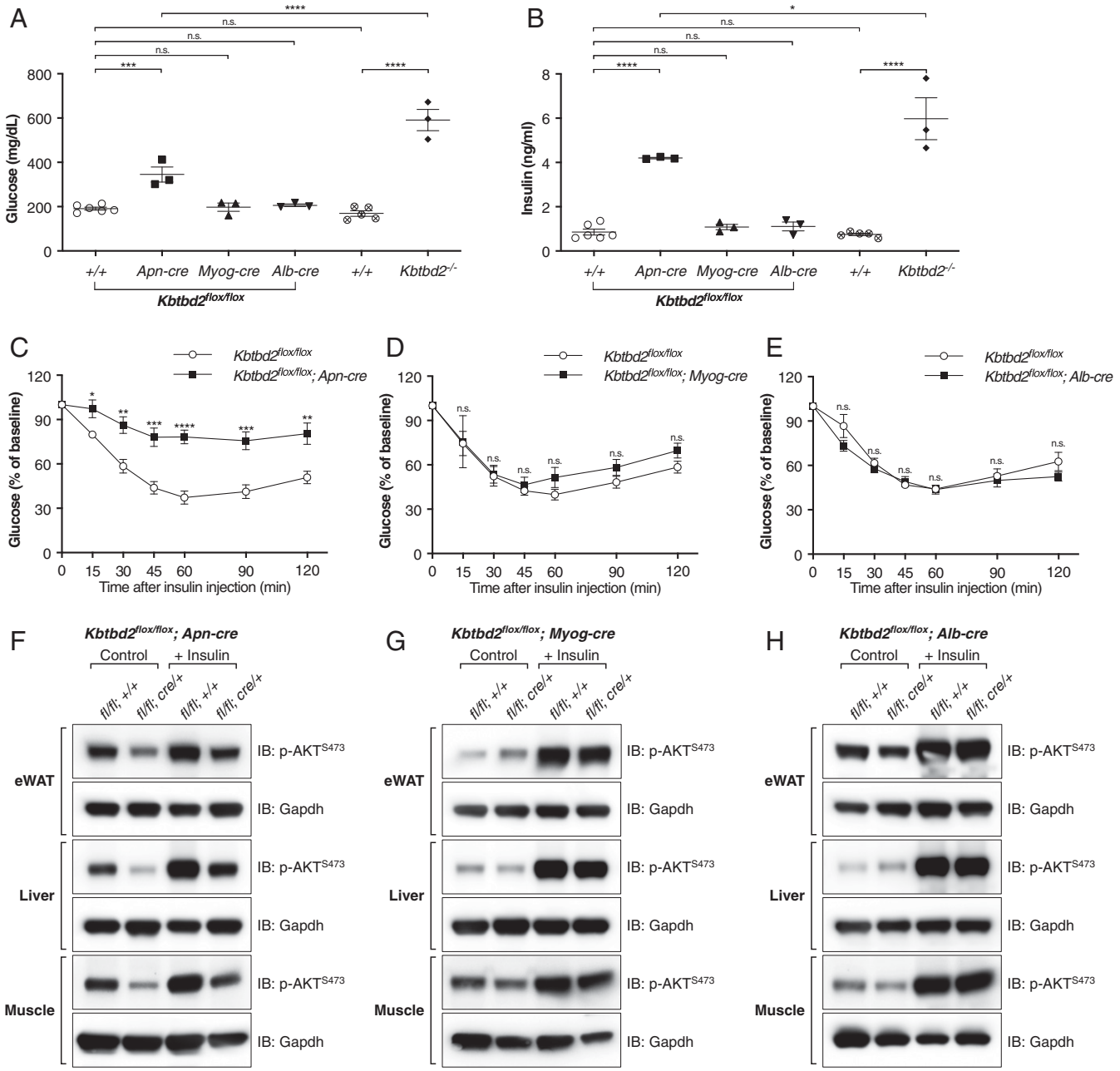

Fig. 4. The regulation of insulin sensitivity by KBTBD2 in adipose tissue, liver, and muscle. (*A* and *B*) Blood glucose (*A*) and serum insulin (*B*) in 8-wk-old male mice after a 6-h fast. (*C*–*E*) Insulin tolerance test. Blood glucose was measured at indicated times after i.p. insulin injection in 12-wk-old male mice [(*C*) n = 8 *Kbtbd2*$^{flox/flox}$, 6 *Kbtbd2*$^{flox/flox}$*;Apn-cre*, (*D*) n = 6 *Kbtbd2*$^{flox/flox}$, 3 *Kbtbd2*$^{flox/flox}$*;Myog-cre*, (*E*) n = 8 *Kbtbd2*$^{flox/flox}$, 5 *Kbtbd2*$^{flox/flox}$*;Alb-cre*]. (*F* and *G*) Immunoblots of different tissue lysates of 12-wk-old male *Kbtbd2*$^{flox/flox}$*;cre* mice and *Kbtbd2*$^{flox/flox}$ littermates 30 min after control or insulin injection. Data are representative of two independent experiments. Data points represent individual mice (*A* and *B*). Data are presented as means ± SEM (*A*–*E*). *P* values were determined by one-way ANOVA with Tukey's multiple comparison test (*A* and *B*) or Student's *t* test (*C*–*E*). *$P \le 0.05$; **$P \le 0.01$; ***$P \le 0.001$; ****$P \le 0.0001$; ns, not significant with $P > 0.05$.

Discussion

In our previous work, the transplantation of WT adipocytes to *teeny* mice of postweaning age was shown to rescue hyperglycemia, insulin resistance, and hepatosteatosis, while failing to correct body length (3). This suggested that KBTBD2 deficiency in adipocytes accounted for most of the *teeny* phenotype, but did not exclude a contribution by other tissues. It was, in fact, notable that total body insulin resistance was fully alleviated by adipose tissue transplantation, given the supposition that insulin signaling in muscle and liver cells, collectively representing a large proportion of total body weight, might still be abnormal. As to the failure of adipocyte transplantation to rescue the shortfall in body length, we reasoned that intervention might have come too late to do so.

To more directly examine the essential functions of KBTBD2 in insulin signaling in other tissues, and to determine whether adipose, muscle, or liver tissue KBTBD2 activity might be independently required for growth, we made use of tissue-specific conditional *Kbtbd2* knockout mutations in the present study. We have also been able to assess the effects of KBTBD2 loss from each of these tissues on the physiology of the other two tissues.

Loss of KBTBD2 in adipocytes causes striking accumulation of p85α in brown and white adipose tissues, and leads to diminution in the quantity of these adipose tissues, as observed in *teeny* mice. It also caused insulin resistance and hyperglycemia. This led to secondary hepatosteatosis, as well as insulin resistance in both liver and muscle cells. In contrast, in the liver-specific *Kbtbd2* knockout mice, we only observed a slightly increased level of p85α, and no significant effect on adipose tissue mass. In the muscle-specific *Kbtbd2* knockout mice, no change at all was observed in the level of p85α, and no effect on adipose tissue mass was observed. Insulin resistance was not evident in any of the three tissues examined, nor systemically. It would appear that when adipocytes exhibit severe insulin resistance and are few in number, as in *teeny* mice or adipocyte-specific *Kbtbd2* knockout mice, excess lipid spills over into the liver. But the converse situation is not observed when KBTBD2 is absent in the liver or muscle; in each case, there is no detectable effect on cell-intrinsic insulin sensitivity, nor on adipose tissue mass.

Adipocyte-specific *Kbtbd2* knockout mice display a reduction of fat mass versus lean body mass, as well as p85α accumulation similar to *Kbtbd2*$^{-/-}$ mice. We also observed a comparable level of liver triglyceride accumulation and liver damage in these mouse models. Despite these similarities, the extent of hyperglycemia and the changes in insulin level are different. *Kbtbd2*$^{-/-}$ mice have a fasting blood glucose of around 600 to 700 mg/dL, while adipocyte-specific *Kbtbd2* knockout mice have a fasting blood glucose of around 300 to 400 mg/dL and no glycosuria even in the fed state. The fasting blood insulin levels of *Kbtbd2*$^{-/-}$ mice increases over time and peaks around 7 wk of age, then declines to near WT levels (3). The fasting insulin level in adipocyte-specific *Kbtbd2* knockout mice remains high at least through 16 wk of age. Pancreatic β cells respond to systemic insulin resistance with increased insulin secretion, which entails expansion of β-cell mass and enhanced β-cell function (8). The rapid reduction of insulin levels in *Kbtbd2*$^{-/-}$ mice beginning at 7 wk of age suggests that exhausted β cells are unable to further produce insulin to decrease the high level of blood glucose. However, the adipocyte-specific *Kbtbd2* knockout mice maintain ample β-cell function until at least 16 wk of age. It is possible that the phenotypic effect of global *Kbtbd2* knockout is more severe than conditional *Kbtbd2* knockout in adipose tissues due to additive effects of metabolic disorders in individual tissues. Alternatively, these differences may be a result of KBTBD2 deficiency within β cells themselves.

The failure of adipocyte-specific knockout of *Kbtbd2* to recapitulate the growth retardation observed in *teeny* mice might be attributable to the importance of KBTBD2 in tissues yet to be examined, and specifically in the preservation of insulin-like growth factor 1 (IGF1) signaling. IGF1 is produced largely by the liver under the influence of pituitary growth hormone and strongly stimulates the growth of most tissues, including bones. IGF1 signaling engages the same PI3K–AKT axis as insulin to elicit biological responses (9). We have earlier observed that IGF1 levels are dramatically elevated in *Kbtbd2*$^{-/-}$ mice (3). We interpret this as a homeostatic accommodation to growth failure and the metabolic changes that accompany it. We further suggest that p85α accumulation interrupts signaling from the IGF1 receptor (IGF1R), just as it interrupts signaling from the insulin receptor. We observed normal body weight and length in mice with isolated deletions of *Kbtbd2* in adipocytes, liver, and muscle (although not in *Kbtbd2*$^{-/-}$ mice). It would be informative to target *Kbtbd2* specifically in bone or cartilage.

Among the advantages of the tissue-specific conditional knockout approach used here, we are able to identify cell-intrinsic and cell-extrinsic effects of gene deletion in a system that is hormonally interconnected. As we have now shown, adipocyte-specific knockout of *Kbtbd2* causes marked systemic insulin resistance. While this is initiated in adipocytes, wherein the insulin signal is interrupted by an excess of p85α, it does not remain restricted to adipocytes. Although genetically normal, muscle and liver also become insulin resistant, as revealed by their failure to phosphorylate AKT at residue S473. It remains to be determined whether resolution of this lesion, either by fat transplantation or by genetic reversion, or by attenuation of insulin production, would reverse insulin resistance in other tissues, and if so, over what time frame. The pathogenesis of insulin resistance has been ascribed to various mechanisms, including ectopic lipid accumulation, unfolded protein response pathway activation, and inflammation (10). Activation of protein kinase C isoforms by hepatic diacylglycerol, as well as increased ceramide levels, have also been proposed to impair insulin signaling (11). These events may eventually lead to modification of key insulin signaling proteins, such as serine/threonine phosphorylation of IRS1 (12). Our adipocyte-specific *Kbtbd2* knockout mice provide a system with which to further explore secondary insulin resistance mechanisms. In any case, it is clear that in mice with an adipocyte-specific *Kbtbd2* knockout, primary insulin resistance in adipocytes becomes generalized through the induction of secondary insulin resistance in both liver and muscle, although neither of these tissues is genetically abnormal. The effects of the adipocyte-specific knockout that we report here could be caused either by the lack of KBTBD2 in mature adipocytes or by a developmental phenotype that prevents adipogenesis from properly occurring.

Kbtbd2 mRNA can be detected in many mouse tissues (3). Despite the presence of both KBTBD2 and p85α in adipose tissues, liver, and muscle, physiologically significant degradation of p85α by KBTBD2 has so far been observed only in adipose tissues. It appears that KBTBD2 becomes necessary for restriction of p85α in mature adipocytes based on the following two observations: in adipocyte-specific *Kbtbd2* knockout mice, p85α only accumulates in isolated floating fat cells, remaining unchanged in the SVF, which contains preadipocytes and immune cells, and mouse embryonic fibroblasts isolated from *Kbtbd2*$^{-/-}$ mice have similar levels of p85α, but p85α only accumulates in mouse embryonic fibroblasts after they are differentiated into adipocytes (3). Further investigation will be needed to understand how and why KBTBD2 differentially degrades p85α in different cells and tissues.

Materials and Methods

Mice. *C57BL/6J* mice (stock#000664), *Apn-cre* mice [*B6.FVB-Tg(Adipoq-cre)1Evdr/J*, stock#028020], and *Alb-cre* mice [*B6.Cg-Speer6-ps1*$^{Tg(Alb\text{-}cre)21Mgn}$*/J*, stock#003574] were purchased from The Jackson Laboratory. The *Myog-cre* mice (6) were provided by Eric Olson (University of Texas Southwestern Medical Center). *Kbtbd2* knockout mice (*C57BL/6J-Kbtbd2*$^{-/-}$) were generated in our laboratory, as previously described (3). *Kbtbd2-floxed* mice (*C57BL/6J-Kbtbd2*$^{flox/flox}$) were generated in our laboratory, using CRISPR/Cas9-mediated gene replacement with the following sgRNAs and oligo templates:

sgRNA#1, 5′-CCGACAGTGCAAATAGTAGC-3′

sgRNA#2, 5′-TGGGTATGACAGTACTCGGG-3′

Oligo#1, 5′-TGGCTCTTTTTAAAAAGGACTTAGTATCTTTGTTTTGTGTGCTGA
GGATATGTGTCCAGGAGCTATGACAGAATCCTGCTGGATCCATAACTTCGT
ATAATGTATGCTATACGAAGTTATACTATTTGCACTGTCGGATTGAAAACA
TTTCTGTTACCTGTTTTCGTGTGTATAGTCATTTCTCATCCCTCCCATAGCTC-3′

Oligo#2, 5′-CACAAGGTCATAATCTGTGTGGGTTTGATTACAGAATTAAAT
TAAAATTAAAAATTAACAAGCTGGGTATGACAGTACTCCTCGAGATAACTT
CGTATAATGTATGCTATACGAAGTTATGGGAGGCTGAGGCAGGAGGAT
CAAAGATTCTCCAGGGCACCCCAAACTGTCTTGAAAGAGACAGAGACA
AATTATGTTTC-3′.

Tissue-specific knockout of *Kbtbd2* was achieved by breeding *Kbtbd2-floxed* mice with mice expressing each *cre* construct. All mice were fed standard chow diet (2016 Teklad Global 16% Protein Rodent Diet) and housed at room temperature (22 °C). Mice were maintained at the University

of Texas Southwestern Medical Center, and studies were performed in accordance with institutionally approved protocols. All experiments in this study were approved by the University of Texas Southwestern Medical Center Institutional Animal Care and Use Committee.

Metabolic Analysis. Mice were fasted for 6 h (7:00 AM to 1:00 PM) for insulin tolerance tests. Blood glucose was tested with the AlphaTRAK glucometer and test strips. After the first blood glucose measurement, the insulin tolerance test was initiated by i.p. injection with human insulin (0.75 U/kg; Sigma-Aldrich) and blood glucose was measured at set times during the next 2 h. For insulin-stimulated AKT activation, insulin or saline was injected i.p. at a dose of 1.5 U/kg body weight after a 6-h fast. Tissues were collected at 30 min postinjection.

Blood/Serum Chemistries, ELISA, Liver Triglyceride Measurement, and Immunohistochemistry. Mice were fasted for 6 h (7:00 AM to 1:00 PM) for all blood sample collections. Enzyme-linked immunosorbent assay (ELISA) kits were used to measure insulin (Crystal Chem) and leptin (Crystal Chem) in the serum, according to the manufacturer's instructions. Serum ALT and liver triglyceride were measured by the University of Texas Southwestern Medical Center Metabolic Phenotyping Core with standard protocols. Samples for histology were harvested from anesthetized mice and fixed according to standard procedures. The staining protocols for H&E staining and Oil Red O staining were described previously (3).

Sample Preparation, DNA Agarose Gel, and Western Blot Analysis. Tissue samples were snap frozen in liquid nitrogen immediately after dissection. Isolation and separation of murine primary adipocytes and SVF cells from iWAT were performed as described previously (13). TRIzol (Invitrogen) reagent was used to isolate genomic DNA and protein from the same sample in a sequential manner following a standard protocol. Genomic DNA was amplified with primers flanking Ex3 and two *Lox*P sites to detect the Ex3 deletion with 1.5% DNA agarose gel. Protein samples were normalized to 4 μg/μL in 1× NuPAGE lithium dodecyl sulfate sample buffer (Life Technologies) with 2.5% (vol/vol) 2-mercaptoethanol (Sigma-Aldrich). For western blots, 5-μL samples (20 μg total protein) were resolved by NuPAGE 4% to 12% (wt/vol) Bis-Tris gels (Thermo Fisher Scientific), transferred to nitrocellulose membranes (Bio-Rad), blotted with the primary antibody at 4 °C overnight and the secondary antibody for 1 h at room temperature, and then visualized by chemiluminescent substrate (Thermo Fisher Scientific). The following primary antibodies were used in this study: rabbit anti-p85α, anti-Gapdh, and anti-pAKT^{S473} (Cell Signaling Technology).

Data Availability. All data generated in this study are included in this published article and the *SI Appendix*.

ACKNOWLEDGMENTS. We thank the Histopathology, Transgenic, and Metabolic Phenotyping Cores of the University of Texas Southwestern Medical Center for assistance with experiments. We thank Dr. Eric Olson at the University of Texas Southwestern Medical Center for kindly sharing the *Myog-cre* mice. This work was supported by National Institutes of Health grants K99 DK115766 (Z.Z.), R01 AI125581 (B.B.), and U19 AI100627 (B.B.) and the Lyda Hill foundation (B.B.).

1. A. Cignarelli *et al.*, Insulin and insulin receptors in adipose tissue development. *Int. J. Mol. Sci.* **20**, E759 (2019).
2. T. Kadowaki, K. Ueki, T. Yamauchi, N. Kubota, SnapShot: Insulin signaling pathways. *Cell* **148**, 624–624.e1 (2012).
3. Z. Zhang *et al.*, Insulin resistance and diabetes caused by genetic or diet-induced KBTBD2 deficiency in mice. *Proc. Natl. Acad. Sci. U.S.A.* **113**, E6418–E6426 (2016).
4. J. Luo, S. J. Field, J. Y. Lee, J. A. Engelman, L. C. Cantley, The p85 regulatory subunit of phosphoinositide 3-kinase down-regulates IRS-1 signaling via the formation of a sequestration complex. *J. Cell Biol.* **170**, 455–464 (2005).
5. J. Eguchi *et al.*, Transcriptional control of adipose lipid handling by IRF4. *Cell Metab.* **13**, 249–259 (2011).
6. S. Li *et al.*, Requirement for serum response factor for skeletal muscle growth and maturation revealed by tissue-specific gene deletion in mice. *Proc. Natl. Acad. Sci. U.S.A.* **102**, 1082–1087 (2005).
7. C. Postic *et al.*, Dual roles for glucokinase in glucose homeostasis as determined by liver and pancreatic beta cell-specific gene knock-outs using Cre recombinase. *J. Biol. Chem.* **274**, 305–315 (1999).
8. M. Prentki, C. J. Nolan, Islet beta cell failure in type 2 diabetes. *J. Clin. Invest.* **116**, 1802–1812 (2006).
9. F. Hakuno, S. I. Takahashi, IGF1 receptor signaling pathways. *J. Mol. Endocrinol.* **61**, T69–T86 (2018).
10. V. T. Samuel, G. I. Shulman, Mechanisms for insulin resistance: Common threads and missing links. *Cell* **148**, 852–871 (2012).
11. R. J. Perry, V. T. Samuel, K. F. Petersen, G. I. Shulman, The role of hepatic lipids in hepatic insulin resistance and type 2 diabetes. *Nature* **510**, 84–91 (2014).
12. Y. Zick, Insulin resistance: A phosphorylation-based uncoupling of insulin signaling. *Trends Cell Biol.* **11**, 437–441 (2001).
13. S. Viswanadha, C. Londos, Determination of lipolysis in isolated primary adipocytes. *Methods Mol. Biol.* **456**, 299–306 (2008).